HHS Public Access

Author manuscript

Stroke. Author manuscript; available in PMC 2015 March 05.

Published in final edited form as:

Stroke. 2014 February ; 45(2): 598–601. doi:10.1161/STROKEAHA.113.003548.

Quantitative Susceptibility Mapping and Dynamic Contrast Enhanced Quantitative Perfusion in Cerebral Cavernous Angiomas

Abdul Ghani Mikati, MD[1,*], **Huan Tan, PhD**[1,*], **Robert Shenkar, PhD**[1], **Luying Li, MD**[1,2], **Lingjiao Zhang, MS**[1], **Xiaodong Guo, PhD**[3], **Changbin Shi, MD, PhD**[1], **Tian Liu, PhD**[5], **Yi Wang, PhD**[6,7], **Akash Shah, MD**[4], **Robert Edelman, MD**[8], **Gregory Christoforidis, MD**[4], and **Issam Awad, MD**[1]

[1]Section of the Neurosurgery, Department of Diagnostic Radiology, The University of Chicago, Chicago, IL

[2]Department of Neurosurgery, West China Hospital of Sichuan University, Sichuan, China

[3]Brain Research Imaging Center, Department of Diagnostic Radiology, The University of Chicago, Chicago, IL

[4]Section of Neuroradiology, Department of Diagnostic Radiology, The University of Chicago, Chicago, IL

[5]MedImageMetric LLC, New York, NY

[6]Department of Radiology, Weill Cornell Medical College, New York, NY

[7]Department of Biomedical Engineering, Cornell University, Ithaca, NY

[8]Department of Radiology, NorthShore University HealthSystem, Evanston, IL

Abstract

Background—Hyperpermeability and iron deposition are two central pathophysiological phenomena in human cerebral cavernous malformation (CCM) disease. Here we used two novel magnetic resonance imaging (MRI) techniques to establish a relationship between these phenomena.

Methods—Subjects with CCM disease (4 sporadic and 18 familial) underwent MRI imaging using the Dynamic Contrast Enhanced Quantitative Perfusion (DCEQP) and Quantitative Susceptibility Mapping (QSM) techniques that measure hemodynamic factors of vessel leak and iron deposition respectively, previously demonstrated in CCM disease. Regions of interest encompassing the CCM lesions were analyzed using these techniques

Results—Susceptibility measured by QSM was positively correlated with permeability of lesions measured using DCEQP (r=0.49, p=<0.0001). The correlation was not affected by factors

Corresponding Author: Issam A. Awad, MD, Section of Neurosurgery, 5841 S. Maryland Ave., Room J325, M/C 3026, Chicago, IL, 60637, USA, Fax: 1-773-702-3518, Tel.: 1-773-702-2123, iawad@uchicago.edu.

*Denote co-authors with equal contributions

Disclosures: None

including familial predisposition, lesion volume, the contrast agent and the use of statin medication. Susceptibility was correlated with lesional blood volume (r=0.4, p=0.0001), but not with lesional blood flow.

Conclusion—The correlation between QSM and DCEQP suggests that the phenomena of permeability and iron deposition are related in CCM; hence "more leaky lesions" also manifest a more cumulative iron burden. These techniques might be used as biomarkers to monitor the course of this disease and the effect of therapy.

Keywords

Quantitative Susceptibility Mapping; Dynamic Contrast Enhanced Quantitative Perfusion; Cerebral Cavernous Malformation; Cavernous Angioma; Magnetic Resonance Imaging; cerebrovascular disease/stroke; cerebrovascular disorder

Introduction

Cerebral cavernous malformations (CCM) are characterized by capillary dilatations with deficient blood brain barrier and disrupted interendothelial tight junctions that may cause vessel hyperpermeability[1–3]. This hyperpermeablity may cause chronic blood leakage with neurologic sequelae including epilepsy and focal deficits, and hemorrhagic stroke. We previously showed that Rho kinase (ROCK) inhibition by Fasudil decreases iron deposition and lesion burden in mouse brain models[4] and mice haploinsufficient in *Ccm* gene demonstrated increased permeability of vessels to Evan's blue dye that is reversible by ROCK inhibition[5].

With the advent of ROCK inhibition as a potential therapy, a method for assessing its effect is needed. Recent advances in magnetic resonance imaging (MRI) have provided two potential methods to accomplish this. The first being Dynamic Contrast Enhanced Quantitative Perfusion (DCEQP) is used to measure hemodynamic parameters such as permeability. Applicability of DCEQP has been demonstrated by Larsson et al.[6], and has subsequently been validated with comparisons to histology[7] and quantitative autoradiography[8]. The second method, Quantitative Susceptibility Mapping (QSM)[9, 10], measures the magnetic susceptibility of the brain tissue, an intrinsic biophysical property of the tissue that is directly proportional to the local iron content. Both methods have been employed in assessing characteristics of CCM lesions in human. Given the common underlying pathophysiological mechanisms of the disease and the potential to use these techniques as biomarkers for disease activity and response to treatment, we hypothesize that there is a positive correlation between permeability measured with DCEQP and iron burden as measured by QSM.

Materials and Methods

Subjects

After obtaining IRB approval and informed consent, 21 patients scheduled for routine clinical evaluation for CCM disease were recruited, including one case that included a

second follow-up scan (characteristics in table 1). These patients were seen regularly in clinic for follow-up of their CCMs.

Data acquisition and Processing

All scans were obtained during regular clinical follow-up. Permeability was measured using a T_1-weighted DCEQP protocol that included a pre-contrast T_1 scan followed by a dynamic scan using gadolinium contrast (gadodiamide or gadobenate dimeglumine). Images were then processed in Matlab using the Patlak mathematical model to calculate permeability, cerebral blood flow and volume (CBF and CBV) maps. Regions of interest (ROIs) were selected encompassing entire lesions as they appeared on T2 weighted images that were acquired simultaneously, and were then superimposed on the maps.

A single three dimensional, multi-echo, T2*-weighted, spoiled gradient echo sequence was used for data collection for QSM reconstruction. The QSM images were reconstructed using customized software employing a morphology-enabled dipole inversion algorithm[11, 12]. ROIs included the same lesions identified on T_2 images used for permeability. More detailed information available in online supplement (please see http://stroke.ahajournals.org).

Statistics

Pearson correlation was used to examine the correlation between QSM susceptibility vs. permeability, CBF and CBV. Multivariate linear regression was used to assess the impact of potential contributing factors on the above-mentioned correlations, with susceptibility as the dependent variable, including permeability, the factor and their interaction in the model. Bland-Altman plots were constructed to evaluate intra-observer and inter-observer consistency, and coefficients of variation were calculated to look at interpatient and intrapatient variability.

Results

Figure 1 shows an example of a T2 image used for ROI selection, as well as a permeability map and QSM image of the same lesion. Intra-observer and inter-observer consistency were demonstrated with both techniques in a subcohort of cases. (please see supplemental results, http://stroke.ahajournals.org). Table 1 illustrates the patients' salient clinical features, and summarizes imaging results for each case with both techniques. A positive correlation was found between mean QSM susceptibility of lesions and mean permeability of the same lesions ($r=0.49$, $p=<0.0001$, Figure 2A). This correlation between susceptibility and permeability was present predominantly in familial cases, and was independent of lesion volume, the contrast agent used and whether the patient was receiving statin therapy (please see supplemental results, http://stroke.ahajournals.org). The correlation persisted when the data from cases with multiple lesions was pooled and averaged in each patient ($r=0.46$, $p=0.038$) (Figure 2B).

There was a positive correlation between susceptibility and CBV in lesions ($r=0.4$, $p=<0.0001$) and no correlation between susceptibility and CBF in lesions ($r=0.1$, $p=0.34$) (please see supplemental results, http://stroke.ahajournals.org). Repeated analyses using

median values of susceptibility and permeability showed similar results (r= 0.4, p=0.0001, data not shown).

Discussion

Vascular permeability is a hallmark or CCM disease, demonstrated as a result of loss of CCM gene expression in cultured endothelial cells and in the skin, lungs and brain of CCM heterozygous mice[5, 13]. It has not been examined systematically in man. Chronic iron deposition is also a cardinal feature of CCM lesions, demonstrated by imaging and histopathology. Here we imaged human CCM lesions using two novel techniques examining permeability and the quantitative burden of iron deposit, respectively. The two techniques measure different and distinct features of the CCM lesion, yet these may be related biologically. We postulated and demonstrated indeed that the more “leaky” CCM lesions also exhibited significantly greater mean susceptibility. This strong correlation was present regardless of lesion volume, two different contrast agents, and whether the patient was using statin, a drug that may impact vascular permeability[14]. The correlation was present mostly in familial cases, representing the vast majority of cases and lesions in our cohort. It will need to be examined in a larger group of sporadic cases. The correlation was present even when multiple lesions per case were averaged and analyzed by subject. Our results establish a proof of concept, and help generate relevant hypotheses about the potential applicability of either technique to monitor CCM lesion behavior. The results may be interpreted using a transport model governed by mass conservation. Hence permeability would reflect current on-going rate of leaking, while susceptibility reflects the integral or historical accumulation of leaking. This and other hypotheses about QSM and DCEQP in CCM will need to be examined in prospective studies.

We noted a range of susceptibility and permeability (as well as CBF and CBV) among CCM lesions. The correlates of this variation will be examined in a larger cohort of cases, including the potential impact of age, lesion features, genotype and prior clinical activity. Internal and external validity, interobserver consistency, and the reproducibility of the measurements will require further validation. Statin use and other therapies can potentially modulate permeability in CCM lesions, and their effects will need more systematic study. Future research will also address the potentially different implications of CBV, CBF, permeability and susceptibility, in lesions themselves and in background brain.

Conclusion

QSM and DECQP are two unique imaging methods for quantitatively assessing CCM biologic behavior. Strong correlation was observed between the two methods for measuring different endpoints of the same pathophysiological phenomena. This serves as proof of concept for these methods and the biological phenomena they measure. It also reflects their potential as biomarkers of CCM disease.

Supplementary Material

Refer to Web version on PubMed Central for supplementary material.

Acknowledgments

Sources of Funding: This work was supported in part by a Collaborative and Translational Studies Award through the Institute of Translational Medicine at the University of Chicago (*UL1 TR000430*), and by the Bill and Judy Davis Research Fund in Neurovascular Research.

References

1. Clatterbuck RE, Eberhart CG, Crain BJ, Rigamonti D. Ultrastructural and immunocytochemical evidence that an incompetent blood-brain barrier is related to the pathophysiology of cavernous malformations. Journal of Neurology, Neurosurgery and Psychiatry. 2001; 71:188–192.
2. Wong JH, Awad IA, Kim J. Ultrastructural pathological features of cerebrovascular malformations: A preliminary report. Neurosurgery. 2000; 46:1454–1459. [PubMed: 10834648]
3. Tu J, Stoodley MA, Morgan MK, Storer KP. Ultrastructural characteristics of hemorrhagic, nonhemorrhagic, and recurrent cavernous malformations. Journal of Neurosurgery. 2005; 103:903–909. [PubMed: 16304995]
4. McDonald DA, Shi C, Shenkar R, Stockton RA, Liu F, Ginsberg MH, et al. Fasudil decreases lesion burden in a murine model of cerebral cavernous malformation disease. Storke. 2012; 43:571–574.
5. Stockton RA, Shenkar R, Awad IA, Ginsberg MH. Cerebral cavernous malformations proteins inhibit rho kinase to stabilize vascular integrity. Journal of Experimental Medicine. 2010; 207:881–896. [PubMed: 20308363]
6. Larsson HBW, Courivaud F, Rostrup E, Hansen AE. Measurement of brain perfusion, blood volume, and blood-brain barrier permeability, using dynamic contrast-enhanced t1-weighted mri at 3 tesla. Magnetic Resonance in Medicine. 2009; 62:1270–1281. [PubMed: 19780145]
7. Hoffman A, Bredno J, Wendland MF, Derugin N, Hom J, Schuster T, et al. Validation of in vivo magnetic resonance imaging blood-brain barrier permeability measurements by comparison with gold standard histology. Stroke. 2011; 42:2054–2060. [PubMed: 21636816]
8. Ferrier MC, Sarin H, Fung SH, Schatlo B, Pluta RM, Gupta SN, et al. Validation of dynamic contrast-enhanced magnetic resonance imaging–derived vascular permeability measurements using quantitative autoradiography in the rg2 rat brain tumor model. Neoplasia. 2007; 9:546–555. [PubMed: 17710157]
9. de Rochefort L, Liu T, Kressler B, Liu J, Spincemaille P, Lebon V, et al. Quantitative susceptibility map reconstruction from mr phase data using bayesian regularization: Validation and application to brain imaging. Magn Reson Med. 2010; 63:194–206. [PubMed: 19953507]
10. Schweser F, Deistung A, Lehr BW, Reichenbach JR. Quantitative imaging of intrinsic magnetic tissue properties using mri signal phase: An approach to in vivo brain iron metabolism? Neuroimage. 2011; 54:2789–2807. [PubMed: 21040794]
11. Liu T, Liu J, Rochefort Ld, Spincemaille P, Khalidov I, Ledoux JR, et al. Morphology enables dipole inversion (medi) from a single-angle acquisition:Comparison with cosmos in human brain imaging. Magnetic Resonance in Medicine. 2011; 66:777–783. [PubMed: 21465541]
12. Liu T, Khalidov I, Rochefort Ld, Spincemaille P, Liu J, Tsiouris A, et al. A novel background field removal method for mri using projection onto dipole fields (pdf). NMR in Biomedicine. 2011; 24:1129–1136. [PubMed: 21387445]
13. Whitehead KJ, Chan AC, Navankasattusas S, Koh W, London NR, Ling J, et al. The cerebral cavernous malformation signaling pathway promotes vascular integrity via rho gtpases. Nature Medicine. 2009; 15:177–184.
14. Liu PY, Liu YW, Lin LJ, Chen JH, Liao JK. Evidence for statin pleiotropy in humans: Differential effects of statins and ezetimibe on rho-associated coiled-coil containing protein kinase activity, endothelial function, and inflammation. Circulation. 2009; 119:131–138. [PubMed: 19075102]

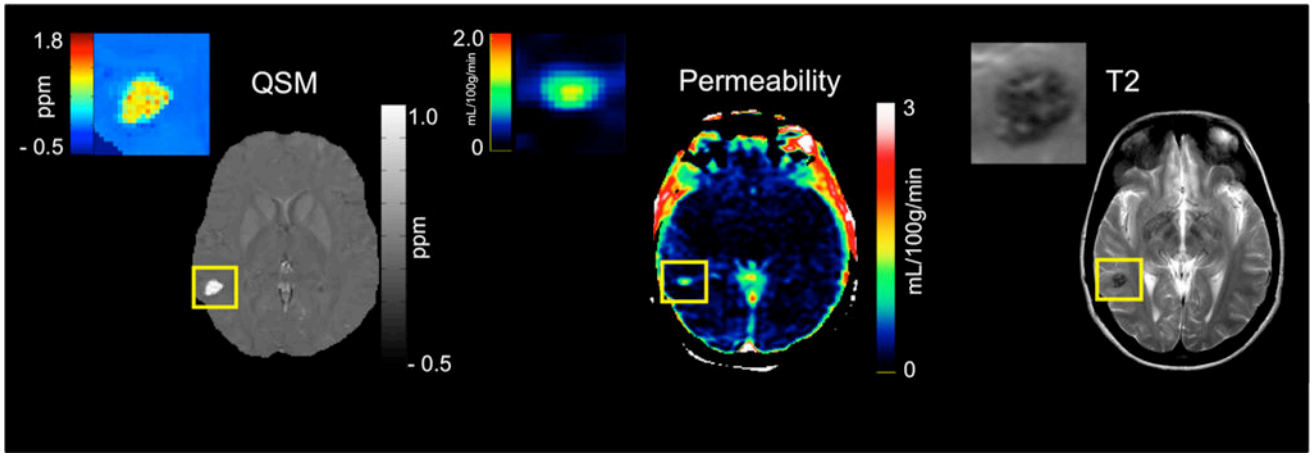

Figure 1. MR Images used for assessing CCM lesions

Left, an example of a QSM image of a sporadic CCM lesion shown as a bright area highlighted within a yellow box. A color-coded map of the lesion itself is shown to indicate the potential distribution of iron within the lesion in parts per million (ppm). Middle, an example of a permeability map of the same lesion generated by MATLAB with areas of high permeability and low permeability indicated according to the color scale to the right of the image with units in ml/100g/min. Right, an example of a T_2 image with the same lesion highlighted within a yellow box.

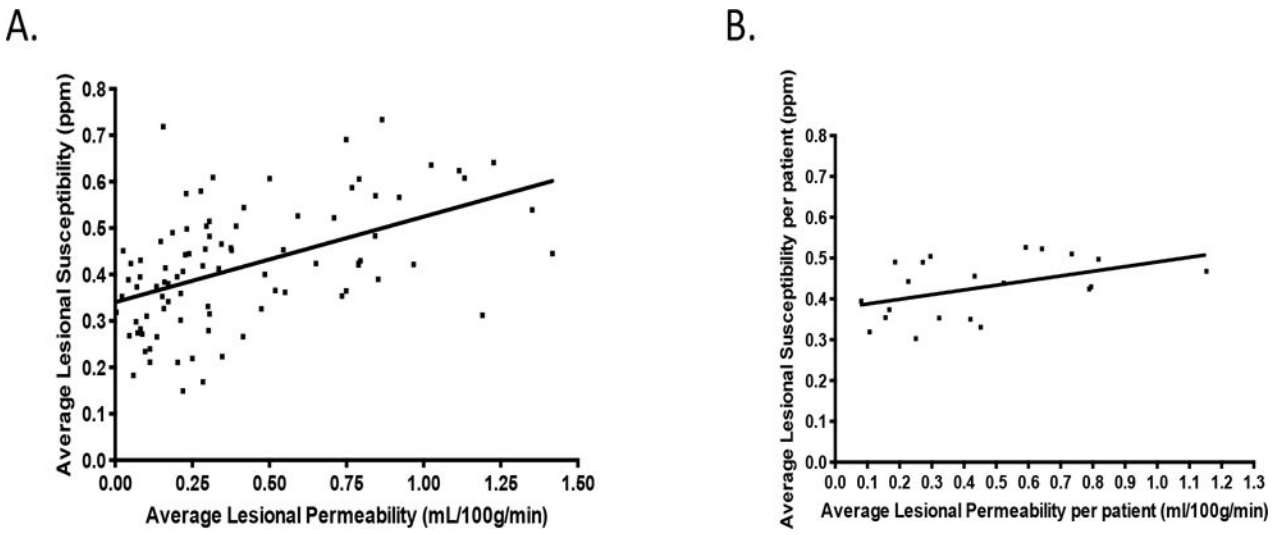

Figure 2. QSM vs. Permeability

A. Scatter plot showing a significantly positive correlation between QSM susceptibility and permeability($r = 0.49$, $p = <0.0001$). B. Scatter plot showing a significantly positive correlation between QSM susceptibility and average permeability per patient ($r = 0.46$, $p = <0.038$).

Table 1

Summary of patient clinical and lesional characteristics.

Patient	Age at scan/gender	Familial Or sporadic	Statin use	Presence of seizures	Hemorrhage within 6 months of Imaging	Contrast used	Number of lesions analyzed	Mean lesional susceptibility (ppm)±mean lesional SD per patient	Mean lesional permeability (mL/100g/min)± mean lesional SD per patient	Average lesional volume per patient (mL)
1	25F	Familial	no	no	no	gadodiamide	7	0.456 ±0.466	0.433 ±0.488	0.99
2	58M	Familial	no	no	no	gadodiamide	16	0.523 ±0.496	0.642 ±0.424	1.008
3	60M	Familial	yes	0	no	gadobenate dimeglumine	1	0.3947 ±0.364	0.081 ±0.088	0.4
4	76F	Familial	yes	no	no	gadobenate dimeglumine	4	0.49 ±0.403	0.272 ±0.142	0.9
5 scan 1	36F	Sporadic	no	no	no	gadobenate dimeglumine	1	0.443 ±0.354	0.227 ±0.226	5.2
5 scan 2	36F	Sporadic	no	no	no	gadodiamide	1	0.5041 ±0.42	0.296 ±0.383	4.4
6	44F	Sporadic	no	no	no	gadobenate dimeglumine	1	0.4297 ±0.33	0.795 ±0.47	0.1
7	11M	Familial	no	no	no	gadobenate dimeglumine	1	0.1685 ±0.113	0.285 ±0.121	0.2
8	14F	Familial	no	no	no	gadobenate dimeglumine	4	0.303 ±0.303	0.251 ±0.143	2.9
9	12F	Familial	no	no	no	gadobenate dimeglumine	8	0.319 ±0.319	0.107 ±0.085	1.3
10	14F	Familial	no	no	yes	gadobenate dimeglumine	2	0.353 ±0.353	0.323 ±0.151	0.32
11	15M	Familial	no	no	no	gadobenate dimeglumine	2	0.51 ±0.51	0.735 ±0.719	2.5
12	40F	Familial	no	no	no	gadobenate dimeglumine	1	0.49 ±0.56	0.186 ±0.221	0.98
13	13M	Familial	no	no	no	gadobenate dimeglumine	5	0.331 ±0.331	0.452 ±0.233	0.79
14	62M	Familial	yes	no	yes	gadobenate dimeglumine	3	0.374 ±0.374	0.168 ±0.103	0.76
15	60M	Familial	yes	no	no	gadobenate dimeglumine	5	0.498 ±0.498	0.818 ±0.600	0.86
16	4M	Familial	no	yes	yes	gadobenate dimeglumine	3	0.35 ±0.35	0.42 ±0.268	2.7
17	34M	Familial	yes	no	no	gadobenate dimeglumine	2	0.468 ±0.468	1.153 ±1.145	9.4
18	32F	Familial	no	no	no	gadodiamide	16	0.354 ±0.354	0.156 ±0.123	0.67
19	42F	Sporadic	no	no	no	gadodiamide	1	0.4243 ±0.344	0.789 ±0.143	0.47
20	40F	Sporadic	yes	no	no	gadobenate dimeglumine	1	0.526 ±0.382	0.592 ±0.346	0.81
21	25F	Familial	no	no	no	gadodiamide	4	0.439 ±0.439	0.524 ±0.378	0.77